Dynamic Stimulated Brillouin Scattering Analysis

A. Djupsjöbacka, G. Jacobsen, and B. Tromborg

***Abstract*—We present a new simple analysis—including the effect of spontaneous emission—of the (dynamic) influence of stimulated Brillouin scattering (SBS) on the detected receiver eye diagram. It applies in principle for general types of modulation formats such as the digital formats of amplitude shift keying (ASK), frequency shift keying (FSK), and phase shift keying (PSK). The analysis is formulated for a determination of the signal power depletion and intersymbol interference (ISI) caused by the combined effect of fiber dispersion, fiber attenuation and nonlinear fiber effects such as the effect of self-phase modulation (SPM) and SBS. The analysis allows a quantification of the dithering influence on the SBS threshold. Representative numerical examples are presented for two single-channel ON–OFF modulated 10-Gb/s systems utilizing Franz–Keldysh and Mach–Zehnder-type modulators.**

***Index Terms*—Nonlinear optics, numerical analysis, optical fiber communication, optical Kerr effect, optical receivers, stimulated Brillouin scattering (SBS), transmission system performance.**

I. Introduction

OPTICAL transmission systems using wavelength-division-multiplexing (WDM) techniques and operating in the 1550–nm fiber transmission window are currently being prototyped for use in the telecom fiber back-bone network. One state of the art research system has a channel bit rate of 160 Gb/s and 19 signal channels for transmission over 40 km of dispersion shifted fiber [1]. Another example system has 64 signal channels (channel bit-rate 10 Gb/s) and transmits over 7200 km of conventional fiber [2].

In the practical design of these WDM systems (and WDM based optical networks) that operates with unrepeated transmission lengths of several hundreds of kilometers it is important to have a rigorous system model that accounts for the linear as well as nonlinear fiber transmission properties as discussed in tutorial format in [3], [4]. The transmission of an ON–OFF modulated signal for a single-channel propagation in the fiber at bit-rates beyond the order of 10 Gb/s is influenced by fiber attenuation and fiber dispersion (including the dispersion slope at the signal wavelength) as well as self-phase modulation (SPM) through the signal intensity dependent fiber refractive index. This is especially the case in applications with cascaded optical amplifiers where the signal power at the amplifier output is above the order of 1 mW (0 dBm). For WDM applications with several optical signal channels separated in frequency by 100–200 GHz the intensity dependence refractive index may in addition lead to cross-phase modulation (XPM) between the signal channels. XPM is especially severe for adjacent channels with the same dispersion value because this allows long interaction lengths between the channels during transmission.

Stimulated Raman scattering (SRS) may cause transfer of signal power among the WDM channels over the total WDM transmission window leading to cross-talk and power depletion effects. The strongest SRS gain is for channels with a relatively large frequency separation (12 THz apart from each other). In a WDM system configuration in the 1550-nm wavelength range SRS leads to power depletion of low wavelength channels and cross-talk induced power enhancement of longer wavelength channels. The SRS effect depends on the dispersion difference between interacting signals (the effective interaction length) in a similar way as XPM.

Another dispersion sensitive nonlinear effect may occur due to four-wave mixing (FWM) effects between adjacent (neighboring) WDM channels. This effect is of special concern for fibers with low dispersion and low dispersion slope (dispersion shifted fibers in the 1550-nm transmission window) [8]. FWM effects have especially severe system quality consequences using WDM channel plans with the same interchannel frequency separation between all channels as described in the ITU recommendations [9].

One last important nonlinear effect that affects the transmission is the stimulated Brillouin scattering (SBS) effect which differs from all the nonlinear effects discussed so far in that the SBS gain profile has a relatively narrow frequency bandwidth (of the order of 100 MHz for typical fibers) meaning that it does not lead to cross coupling effects among WDM signal channels. The SBS leads through the interaction between an optical pump signal and an acoustic wave in the fiber to a the set-up of a counter propagating stimulated (Stokes) wave which is downshifted 11 GHz in frequency relative to the pump. The other stimulated nonlinear processes (FWM, SRS) are broad-band processes [bandwidths in the range of hundreds of GHz (FWM) to the order of 12 THz (SRS)] where the stimulated waves are copropagating with the pump signal(s).

The dynamic properties for the transmitted optical signals are in principle described by the time dependent Maxwell equations which—using an equivalent baseband formulation—leads to modified forms of the Schrödinger equations [3]. The equations have a particular simple form (accounting for the lowest order nonlinear influence) when dealing with time scales above the order of 1–10 ps—as is of interest in this paper—whereas they are of significantly more involved form when dealing with femtosecond time scales [3]. From numerical solutions of the Schrödinger

Manuscript received May 3, 1999; revised December 1, 1999.

A. Djupsjöbacka and G. Jacobsen are with Ericsson Telecom AB, Stockholm S-126 25, Sweden.

B. Tromborg is with the Research Center COM, Technical University of Denmark, Lyngby DK-2800, Denmark.

Publisher Item Identifier S 0733-8724(00)02194-0.

equations the time domain properties of a received optical signal can be specified—for instance by looking at the resulting eye diagram. A practical evaluation accounting for effects of SPM, XPM, SRS, and FWM is in principle straightforward because all optical signals that are injected into the transmission fiber or are generated in the stimulated processes are co-propagating and thus interacts "on the fly," i.e., the resulting optical signal amplitude and phase at a given time and specified fiber position are uniquely determined by all other signals specified at that time instant and at that fiber position. The influence of the SBS process is more complicated because it involves a long SBS interaction time relative to the bit period and because the counter propagation of the stimulated wave relative to the signal which means that a long bit-sequence has to be considered when evaluating the dynamic influence of the SBS on the detected eye diagram.In this paper, we will present a new simplified formulation of the SBS problem for a high bit rate application which allows a quantification of the SBS influence on the detected eye diagram. In order to make the current presentation clear and straightforward we will focus our attention on the single-channel case in the mathematical formulation of the modified Schrödinger equation and in our numerical examples. This means that we will not explicitly consider XPM, SRS, and FWM effects. It should however be noted that our formulation can be modified in a straightforward way to include these effects in a WDM case.

II. Theoretical Outline

A. The Continuous-Wave (CW) Case

1) Our Simplified Model: As a start in our theoretical treatment, we will consider a CW-signal case where a coherent pump wave is injected into the transmission fiber with the (cyclic) carrier frequency ω_c, at the transmission distance $z = 0$ and with intensity $I_p(0)$. In reality the formulation holds for a CW laser pump signal which has a linewidth (caused by phase noise) less than the SBS bandwidth which is about 100 MHz. Thus, the formulation applies for all practical distributed feedback (DFB) laser sources which have typical linewidths in the order of a few MHz. The resulting signal propagation through the fiber to the transmission distance $z = L$ is determined through two nonlinear coupled differential equations. The precise form of the equations depends upon the relative polarization states of the pump and stimulated (Stokes) waves. In the following we present equations for the case where the polarization states are the same for the two waves. This represents a worst case description of the SBS influence. In the situation above the SBS threshold this description is however expected to closely represent the real situation for an installed transmission fiber (i.e., with bends where the bending radius is significantly larger than the 10-cm range). This is because the major interaction between the pump and the Stokes waves happens close to the entrance of the transmission fiber (i.e., within a fiber length where the polarization state of the pump wave is essentially constant).[1] The equations read

$$\begin{cases} \dfrac{dI_p}{dz} = -\dfrac{g_B}{A_{\text{eff}}} I_p I_s - \alpha I_p - \beta_i I_p \\ \dfrac{dI_s}{dz} = -\dfrac{g_B}{A_{\text{eff}}} I_p I_s + \alpha I_s - \beta_i I_p. \end{cases} \tag{1}$$

Here the fiber attenuation is described via the parameter α and the resulting SBS process is specified via the gain g_B (measured relative to the effective fiber core area A_{eff}) and the spontaneous emission factor β_i which accounts for the (Stokes) wave generation occurring throughout the fiber and originating mainly from spontaneous Brillouin scattering from thermally excited sound waves. $I_p(z)$ specifies the intensity in the pump signal which is injected into the fiber at $z = 0$. $I_s(z)$ describes the generated and counter propagating stimulated wave (Stokes wave) which is due to the SBS process. Equation (1) (omitting the spontaneous emission terms) originates from [10] where it is formulated for light propagation in liquids and is given in [3], [4] for the optical fiber case. We have corrected the last formulation by including the normalization for the fiber core area. One should note that the spontaneous emission term in the pump signal equation is insignificant relative to the contribution due to fiber attenuation. The term is included here in order to give a mathematically consistent model. The spontaneous emission term is more significant as far as the Stokes signal equation is concerned. Here it is mandatory to include in order to describe the on-set of the SBS process in a physically correct way.

Note that—although this is not explicitly shown in (1)—the carrier frequency of I_s is downshifted due to conservation of momentum in the SBS process by the acoustic wave frequency of around 11 GHz.

The form of (1) shows that a direct numerical solution is possible. This allows a straightforward numerical implementation in a form which is compatible with our (dynamic) solution of the Schrödinger pump signal equation that will be derived in Section II-B.

2) Discussion of Alternative CW Models Relative to Our Approach: In [5] a more rigorous formulation of the CW SBS problem is given (on an electromagnetic field basis) based upon three coupled first-order differential equations for the pump signal, the stimulated signal and the acoustic wave field. This model is mathematically much more involved than our approach. This rigorous formulation includes the effect of spontaneous emission (earlier theoretical work in this area is found in [6]) but requires—as our model formulation does—separate input data for the spectral SBS gain profile. The spontaneous emission factor is determined from known physical and material parameters for the fiber. The model includes the influence

[1]For input pump powers around or below the threshold the coupling to the Stokes wave occurs over longer fiber lengths and the assumption of constant (relatve) polarization state over time (or distance) is questionable. The effect of the polarization variation may be taken into account by multiplying in (1) the SBS gain g_B by a constant γ which varies between 0.5 (random polarization) and 1 (constant polarization) [3]. In our model we have chosen $\gamma = 1$ in all cases because we will focus on situations of interest for practical optical communication system performance (i.e. pump powers close to or above the SBS threshold).

of polarization effects. The resulting differential equations gives the SBS threshold value and specifies the pump depletion and the Stokes wave generation caused by the SBS process. The numerical solution of the equations is feasible for maximum fiber lengths of about 1 km (which is a short length compared to lengths of interest for the current problem). Longer lengths may be considered using in the model the approximation of considering shorter effective lengths combined with a higher fiber attenuation (corresponding to that of the actual fiber).

Our more approximate formulation does not specify the spontaneous emission parameter from first principles and does not include polarization effects. We end up with a mathematically much simpler CW model where we need to specify the SBS threshold and the SBS bandwidth as input parameters to the calculation (and to adjust the spontaneous emission factor to match the selected SBS threshold—see the discussion in Section V). Results using our model describe the typical SBS behavior (pump depletion and Stokes wave generation) of importance for optical communication systems remarkably well for input pump powers below, around and above the SBS threshold. Furthermore, the analytical (and numerical) formulation is easy to evaluate for transmission lengths of practical interest (in the order of 100 km) and it allows in a straightforward way the modeling of the dynamic SBS problem as it will be shown in Section II-B.

An analytical solution to (1) (in the absence of spontaneous emission) is presented in [3]. In [7] it is pointed out that this solution is erroneous. An exact solution is given in [7] in terms of an integral equation. The solution could not be expressed in closed form using tabulated standard functions, i.e., it requires a numerical evaluation. A major draw back with the CW SBS model that does not account for spontaneous Stokes wave generation is that—in order to describe the on-set of the SBS process—an artificial Stokes signal must be injected at the end of the modeled fiber in the opposite direction of the pump.

B. The Dynamic Pump Wave Model

We now proceed to the dynamic model. In order to move on to a dynamic Schrödinger type of formulation for the signal (pump) we transfer (1) to a set differential equations for the pump and Stokes signal *amplitudes*. We further assume—as an initial step toward the time dependent formulation—that the signal is specified via an average amplitude spectrum $A_p(\omega, z)$ where ω denotes the (cyclic) optical frequency parameter and the spectrum is specified over a "long" bit-sequence. $A_p(\omega, z)$ is in the discussion that follows assumed to have a dominating carrier component.[2, 3] Furthermore, we assume that $A_s(z)$ is a CW signal and contains only one wavelength (11 GHz downshifted relative to the carrier component of $A_p(\omega, z)$). This leads to

$$\begin{cases} \dfrac{\partial A_p(\omega,z)}{\partial z} = -\dfrac{\alpha}{2}A_p(\omega,z) \\ \qquad\qquad - \dfrac{g_B}{2A_{\text{eff}}}A_p(\omega,z)|A_s(z)|^2\delta(\omega-\omega_c) \\ \qquad\qquad - \dfrac{\beta_i}{2}A_p(\omega,z) \\ \dfrac{\partial A_s(z)}{\partial z} = \dfrac{\alpha}{2}A_s(z) \\ \qquad\qquad - \dfrac{g_B}{2A_{\text{eff}}}|A_p(\omega_c,z)|^2 A_s(z) \\ \qquad\qquad - \dfrac{\beta_i|A_p(\omega_c,z)|^2}{2A_s(z)} \end{cases} \tag{2}$$

where ω_c denotes the carrier frequency.

In (2) we have included the effective SBS bandwidth by assuming that the SBS gain only affects the carrier wave.[4] The form of the spontaneous emission term in the Stokes signal equation in (2) shows that this contribution is most significant when the Stokes signal is weak, i.e., in the situation where the spontaneous emission initiates the Stokes signal generation. In this case the term must be treated with special care in order to avoid numerical instabilities in connection with imposing the (Neuman type) boundary condition of $A_s(z) \to 0$ for $z \to L$, where L denotes the length of the transmission fiber.

The spontaneous emission is a stochastic process which can be described by a term $A_p(\omega_c, z)N(z,t)$ in the time domain equation for $A_s(z,t)$ [5]. The factor $N(z,t)$ represents the random fluctuations of density. By assuming $N(z,t)$ to be a Langevin noise function which satisfies the correlation relation

$$\langle N(z,t)N(z',t)\rangle = \beta_i\delta(z-z')$$

the equation for $A_s(z,t)$ is consistent with the Stokes signal equation for the intensity (1). However, for the present problem it will be very demanding in terms of computation time to simulate a Langevin noise function, and we shall therefore stick to the deterministic form (2), which is expected to model the average behavior to a good approximation.

In order to proceed to the general time varying case with a specified bit-pattern for the signal equation [i.e., the top equation in (2)] we now modify it to read in a general operator form (where the signal amplitude may be specified in the time or the frequency domain according to computational convenience):

$$\frac{\partial A_p}{\partial z} = (\bar{D} + \bar{N} + \bar{S})A_p \tag{3}$$

[2]It is possible to consider modulation formats that lead to an average spectrum $A_p(\omega, z)$ with significant discrete components away from the carrier (this happens for instance in the digital frequency shift keying (FSK) case with modulation index values m close to being integer ($m \approx 1, 2, \ldots$) [11]). The current formulation may be modified to cover the SBS influence in such cases. This is discussed in Section III.

[3]Due to the chosen modulation format the "discrete" peaks in the average spectrum $A_p(\omega, z)$ may become broadened (this happens for instance in the digital frequency shift keying (FSK) case with modulation index values close to being half-integer ($m \approx 0.5, 1.5, \ldots$) [11]). In order to account for this the effective peak intensity integrated over the (~100 MHz) bandwidth of the SBS process accounts for the SBS effect—see the discussion in Section IV dealing with the effect of dithering a truly discrete carrier component.

[4]It is worth noting that the influence of SBS is completely determined from the resulting carrier amplitude. This means, for instance, that using duobinary modulation the suppression of the carrier will lead to a significantly enhanced SBS threshold (specified in terms of mean transmitted signal power) as it is well known [12].

which is a generalization of the classical split-step presentation of the Schrödinger equation. It is given here in terms of the dispersion operator $\bar{D}$, a nonlinear fiber operator $\bar{N}$ and an SBS operator $\bar{S}$. Each operator acts upon the signal A_p one by one in the numerical solution of the equation. The evaluation is conveniently done using Fourier transformation techniques by invoking $\bar{D}$ in the frequency domain, $\bar{N}$ in the time domain and $\bar{S}$ in the frequency domain (to specify the depletion of the carrier signal component). The formal operator definitions are

$$\begin{cases} \bar{D} = -\dfrac{\alpha}{2} - j\left(\dfrac{\beta_2}{2}\omega^2 + \dfrac{\beta_3}{6}\omega^3\right) \\ \bar{N} = -j\gamma|A_p|^2 \\ \bar{S} = -\dfrac{g_B}{2A_{\text{eff}}}|A_s(z)|^2\delta(\omega-\omega_c) - \dfrac{\beta_i}{2} \end{cases} \tag{4}$$

where

$$\begin{cases} \beta_2 = -\dfrac{D\lambda^2}{2\pi c} \\ \beta_3 = \dfrac{\lambda^3}{(2\pi c)^2}(\lambda D' + 2D) \\ \gamma = \dfrac{2\pi n_2}{\lambda A_{\text{eff}}} \end{cases} \tag{5}$$

where D denotes the fiber dispersion, D' the dispersion slope, n_2 the nonlinear part of the fiber refractive index (D, D' and n_2 specified at the transmission wavelength λ) and c the free space velocity of light.[5]

In (3), the strength in the SPM process is determined through the signal intensity. Thus

$$|A_p|^2 \equiv |F^{-1}\{A_p(\omega,z)\}|^2 \tag{6}$$

where F^{-1} denotes Inverse Fourier transformation.

The amplitude spectrum is specified from the type of modulation as well as the bit-sequence under consideration. The general formulation which is outlined here thus applies for general modulation formats including the classical digital amplitude shift keying (ASK), frequency shift keying (FSK) and phase shift keying (PSK) formats. In the examples to be considered in the following we focus on ASK generated using a Franz–Keldysh and Mach–Zehnder type of external modulator [13], [14]. The bit-sequence is specified in periodic form, i.e., using a pseudo-random bit-sequence (PRBS) of length $2^N - 1$ bits (N denotes the order of the PRBS sequence).

In the practical numerical solution of the problem, the SBS process is initially solved in the CW domain acting on the carrier only. The coupled differential equations that are used initially are as follows:

$$\begin{cases} \dfrac{\partial A_p(\omega_c,z)}{\partial z} = -\dfrac{\alpha}{2}A_p(\omega_c,z) \\ \qquad\qquad - \dfrac{g_B}{2A_{\text{eff}}}A_p(\omega_c,z)|A_s(z)|^2 \\ \qquad\qquad - \dfrac{\beta_i}{2}A_p(\omega_c,z) \\ \dfrac{\partial A_s(z)}{\partial z} = \dfrac{\alpha}{2}A_s(z) \\ \qquad\qquad - \dfrac{g_B}{2A_{\text{eff}}}|A_p(\omega_c,z)|^2A_s(z) \\ \qquad\qquad - \dfrac{\beta_i|A_p(\omega_c,z)|^2}{2A_s(z)} \end{cases} . \tag{7}$$

Here, the CW solution is only used to calculate $I_s(0) \equiv A_s(0)^2$ from a given value of the input power $I_p(0) \equiv A_p(\omega_c,0)^2$ (and for a value of β_i which is determined from the SBS calibration procedure—see Section V). The benefit is that the differential equation can be solved entirely in the frequency domain which is much faster than a full split-step approach. When the $I_s(0)$-value has been calculated, we use the nonlinear Schrödinger equation for $A_p(\omega,z)$ which is given below to calculate $A_p(\omega,L)$ (at the far end of the fiber, i.e., for $L = 50$, km in the examples to be discussed in Section VI):

$$\begin{cases} \dfrac{\partial A_p(\omega,z)}{\partial z} = (\bar{D}+\bar{N}+\bar{S})A_p(\omega,z) \\ \dfrac{\partial A_s(z)}{\partial z} = \dfrac{\alpha}{2}A_s(z) \\ \qquad\qquad - \dfrac{g_B}{2A_{\text{eff}}}|A_p(\omega_c,z)|^2A_s(z) \\ \qquad\qquad - \dfrac{\beta_i|A_p(\omega_c,z)|^2}{2A_s(z)} \end{cases} \tag{8}$$

where it has been taken into account in the formulation that only the carrier component of the pump signal contributes to the generation of the Stokes signal.

A more rigorous (and ambitious) evaluation approach for the model discussed here is to use the nonlinear Schrödinger equation for $A_p(\omega,z)$ even in the first phase when $I_s(0)$ is calculated. However, for most realistic solutions the differences between these two methods are quite small as will be shown by an example in the Section V.

C. The Fully Dynamic SBS Model

The transient SBS analysis can be presented in a form which is principally more rigorous than the present in terms of three coupled differential equations, one [Schrödinger type—see (8)] for the pump wave, a similar one for the stimulated wave and an equation that describes the acoustic wave (see [3, Section 9.2.4], [15] and [16]). Thus the pump, stimulated and acoustic wave are all treated fully dynamically.

A complete numerical solution of the three coupled equations is extremely difficult. A significant problem arises because the time resolved Stokes wave that originates at the fiber input is caused by the pump wave over the total SBS interaction length of the fiber, i.e., over the order of 20 km (corresponding to contributions from about 10^5 bit-periods of the signal at 10 Gb/s).

[5]The split-step dispersion operator $\bar{D}$ has been given in a form which applies for normal single mode fibers (where the influence of the parameter D dominates compared to the influence of D') as well as for dispersion shifted fibers (with $D \approx 0$ i.e. the influence of D' is important).

Our current dynamic formulation simplifies the evaluation significantly by grasping the main physical effect of the SBS—namely, the depletion of the signal carrier wave—in this way avoiding the need for an equation for the acoustic wave altogether as well as avoiding a dynamic and time resolved evaluation of the stimulated wave evolution.

III. Influence of Additional Discrete Sidebands

In special signal modulation cases the mean amplitude spectrum may contain sidebands that each have a power that exceeds the SBS threshold. In cases where the sidebands are closer to the carrier than the SBS bandwidth they have to be included in the effective carrier pump power in order to determine the effective carrier depletion as discussed in the previous section. In cases where the sidebands are separated by frequencies that are more than the SBS bandwidth each sideband is influenced separately by the SBS and the power depletion can be accounted for by considering each sideband separately.

IV. Dithering

It is well known that by making a periodic modulation of the signal carrier with a spectral width $\omega_m/(2\pi)$ which is larger than the bandwidth $\omega_B/(2\pi)$ of the stimulated Brillouin process (but much lower than the bit rate) the SBS effect is reduced. In a simple conceptual way this type of dithering modulation may be seen as leading to a Lorentzian type carrier wave with a (cyclic) specified half width which is determined by the spectral width parameter ω_m. The relative effective signal carrier power which is influenced by the SBS process may be evaluated as

$$\frac{2}{\pi}\arctan\left(\frac{\omega_B}{\omega_m}\right). \tag{9}$$

The effect of dithering of the carrier wave may now be included in the description of the previous sections by multiplying the SBS gain g_B in (1), (2), (4), (7), and (8) by the quantity specified in (9).

V. Calibration Considerations

The calibration of the SBS process is performed in the way it was discussed for the CW case (Section II-A2). We calibrate the solution relative to an SBS threshold value for a CW-pump wave. Within the mathematical framework discussed here the calibration is done considering a total fiber length L and requiring that $I_s(L) = 0$. This, in turn, allows a specification of the SBS threshold power by adjusting the spontaneous emission parameter β_i. In this paper, we define the threshold input power $I_p(0)$ as the one where the resulting output stimulated signal power is 10 dB below, i.e., $I_s(0) = 0.1 \times I_p(0)$.

In the following examples, we consider a basic 10-Gb/s single-channel system configuration as specified in Table I. The fiber and SBS parameters α, D, D', n_2, A_{eff}, g_B, and ω_B are considered as typical for a normal single-mode fiber whereas β_i has been specified to give an SBS threshold of 0 dBm (1 mW) which we consider a typical value for such fibers.

In Fig. 1, we show—based on the solution of (7)—the pump power (i.e., the power in the signal carrier) as a function of transmission distance as full curves and the stimulated power as dashed curves. The figure is for input CW powers of 10, 7, 3, and 0 dBm. From the figure, it appears that for transmission

TABLE I
Parameters Used in the Simulations

Parameter	Symbol	Value	Unit
Bit-rate	-	10	[Gb/s]
Transmission wavelength	λ	1550	[nm]
PRBS order	N	10	-
Loss parameter	α	0.25	[dB/km]
Dispersion	D	17	[ps/nm/km]
Dispersion slope	D'	0.05	[ps/nm^2/km]
Non-linear index	n_2	2.6	$\times 10^{-20}$ [m^2/W]
Effective area	A_{eff}	80	$\times 10^{-12}$ [m^2]
SBS gain	g_B	5	$\times 10^{-11}$[m/W]
SBS bandwidth	$\omega_B/(2\pi)$	100	[MHz]
Spontaneous emis-. sion parameter	β_i	4.296	$\times 10^{-8}$[m^{-1}]
Total fiber length	L	50	[km]
Rx 3 dB (noi-se) bandwidth	-	7.5 (7.8)	[GHz]

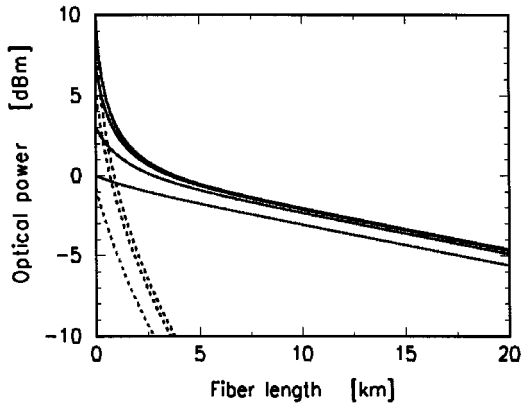

Fig. 1. Pump (full curves) and stimulated power (dashed curves) as a function of transmission distance. Different full curves are for input powers (i.e. power at zero fiber length) of 10, 7, 3, and 0 dBm. (Stimulated wave powers are larger than -10 dBm only for input powers of 10 (upper dashed curve), 7 and 3 dBm and fiber lengths of less than a few kilometers.)

lengths larger than about 5 km the pump power decrease is entirely determined by the fiber attenuation and the transmitted power level saturates due to the SBS generation throughout the initial fiber length. For shorter distances we have an SBS influence which leads to a faster pump power decay and which is more pronounced for the higher input powers as can also be seen from the stimulated signal power curves. We observe a clear influence of SBS for the input pump powers of 3 dBm and above.

In order to further investigate the SBS model we show in Fig. 2 the pump and stimulated power dependences for input carrier powers of 10, 0, -10, and -20 dBm. The figure shows results for the total fiber length of 50 km where Fig. 1 only displays results for the initial 20 km of transmission length (in order to show more clearly the SBS generation for high input powers close to the entrance of the fiber). In Fig. 2, it appears that the stimulated signal power close to the total transmission length of $L = 50$ km is dominated by spontaneous emission (observe the Stokes signal power decrease between 45 and 50 km of transmission distance) whereas for shorter fiber lengths there is a balance between SBS gain, fiber attenuation and spontaneous emission. Close to the fiber entrance there is a sharp increase in stimulated signal power for cases above or close to the SBS threshold of 0 dBm.

The discussion of the CW SBS problem is conveniently summarized in Fig. 3 which shows—based upon the previous figures—the Stokes power and the transmitted pump power as a function of the input pump power. It is obvious how the Stokes wave power grows and the transmitted power saturates above the SBS threshold (0 dBm).

In the examples to be considered in the following the influence of SBS is treated relative to the CW calibration presented in Figs. 1, 2, and 3. This is done by first specifying the mean power injected into the transmission fiber. Secondly the average amplitude spectrum $A_p(\omega, 0)$ is evaluated and the power in the carrier component (for $\omega = \omega_c$) is used as the power that determines the SBS influence using (7). This determines the initial condition [i.e., the value of $A_s(0)$] which is used in the full solution of the Schrödinger Equation (8) when the final eye diagrams are evaluated.

We have finally compared a solution of the SBS calibration problem considering the simple carrier description (7) as well as the full Schrödinger Equation (8) for the case specified in Table I. In Section VI we show in Fig. 8 a typical resulting detected eye diagram which is evaluated (using the CW calibration result for the SBS influence that was discussed above) for an (average) input power of 10 dBm and using a Mach–Zehnder amplitude modulator in the transmitter. The figure will be discussed in detail in Section VI. As a calibration reference, we show in Fig. 4 the difference between this eye diagram and the one which is obtained using the full Schrödinger equation in the calibration of the SBS threshold. It is obvious that the difference in results is less than 0.2% of the eye opening and thus is not significant and we have chosen to utilize the CW calibration throughout our calculations. (We have in our numerical examples tested the model for input power levels up to 20 dBm and have found that using the CW calibration method gives similar accuracy as depicted in Fig. 4 in all cases and speeds up our numerical calculations by about a factor of 15.)

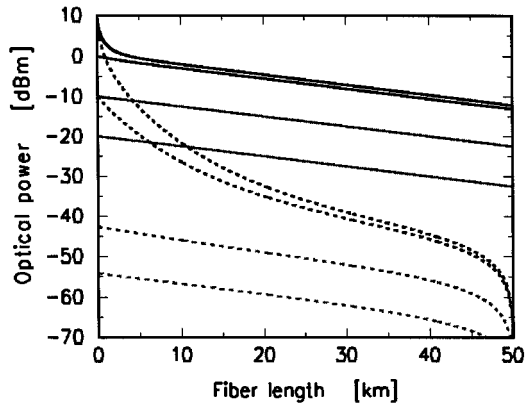

Fig. 2. As Fig. 1 for input powers of $10, 0, -10$, and -20 dBm.

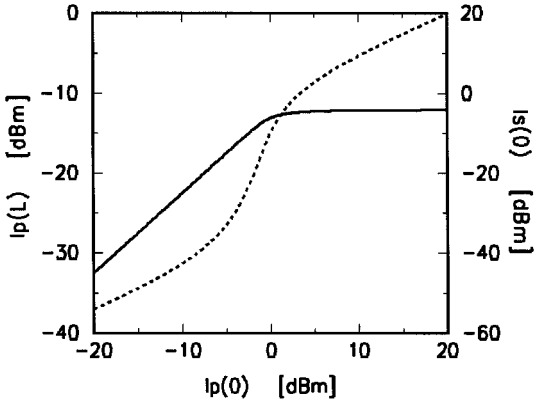

Fig. 3. Transmitted pump power, $I_p(L)$ (full curve—left hand y-axis) and Stokes power, $I_s(0)$ (dashed curve—right hand y-axis) as a function of input pump power, $I_p(0)$ for a fiber with an SBS threshold of 0 dBm.

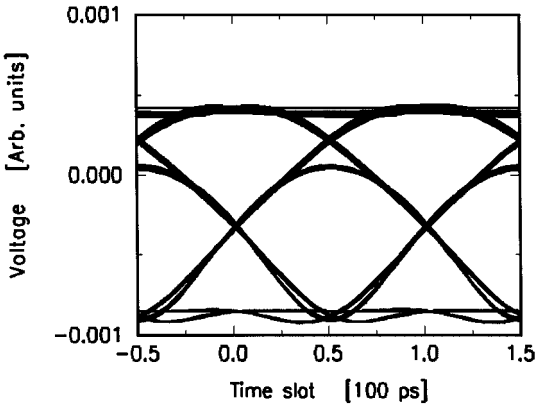

Fig. 4. Difference between the CW-SBS and Schrödinger-SBS solution for the 10-dBm example of Fig. 8.

VI. Numerical Results

In the following, we consider eye diagrams that are obtained detecting ON–OFF modulated digital signals using a photo detector with infinite bandwidth and a fourth-order Bessel–Thompson filter with a 3-dB bandwidth of 7.5 GHz and a noise bandwidth of 7.8 GHz. On the transmitter side a nonfiltered nonreturn-to-zero (NRZ)-signal with raised-cosine flanks were used as input signal to the optical modulators. The modulators were modeled with realistic chirp, but otherwise considered as ideal. The bit-sequence used was a PRBS-10

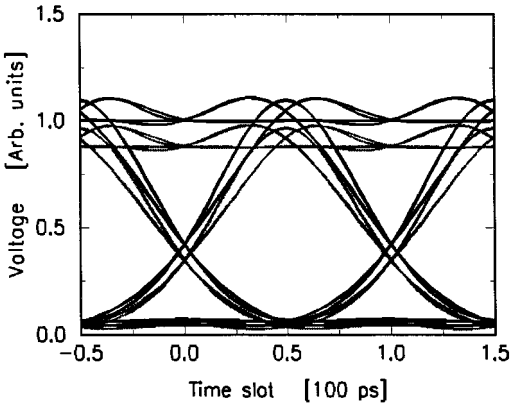

Fig. 5. Detected eye diagram after 50-km transmission using a Franz–Keldysh absorption modulator and for an avarage input power of 2 dBm. Black (gray) curves are without (with) SBS influence.

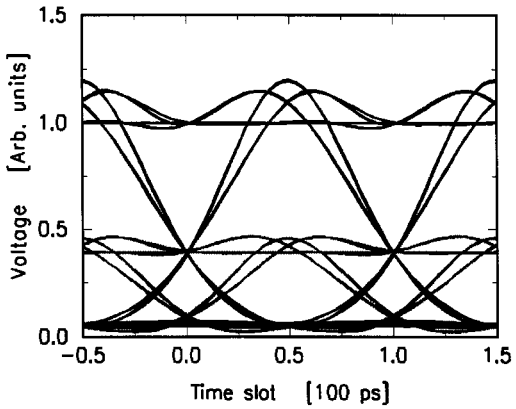

Fig. 6. Same as Fig. 5 for an average input power of 10 dBm.

pattern, i.e., $2^{10} - 1$ bits. The eye diagrams show the influence of ISI effects but do not display the influence of additive noise contributions due to, for instance, amplified spontaneous emission noise, shot noise and thermal noise. The optimum noise bandwidth for the receiver in order to yield the best bit-error ratio performance is around 7.5 GHz (depending on the spectral shape of the noise limiting filter). Here, we have chosen a Bessel–Thompson filter according to the ITU recommendation for eye diagram measurements [9] and scaled it to a 10-Gb/s (STM-64/OC-192) system. We have done that in order to display as clearly as possible the influence of SPM and SBS effects on the detected eye.

In Fig. 5, we show the resulting eye diagram after transmission over 50 km of fiber in the case without (black curves) and with influence of SBS (grey curves) for an (average) input power of 2 dBm. The modulation is in this case accomplished using a typical 10-Gb/s Franz–Keldysh type of external modulator which gives a resulting time dependent signal chirp in combination with the non ideal amplitude (in reality intensity) modulation which also has a finite extinction ratio [13]. The eye is normalized relative to the situation without any SBS influence. The signal is influenced by SPM as well as SBS. It is obvious that we have a small effect of the SBS which is to reduce the effective detected signal amplitude (eye opening) whereas the shape of the eye does not change in any significant way.

In Fig. 6, we show the resulting eye diagram after transmission over 50 km of fiber in the case of an input power of 10 dBm. The distortion of the top part of the eye in the case without SBS which is seen when comparing to the previous figure is due to enhanced SPM influence at 10 dBm input power. It is obvious that we have a significant effect of SBS which is to reduce the effective signal amplitude (eye opening) whereas the shape of the eye does not change very much.

In Figs. 7 and 8, we consider the case of using a Mach–Zehnder type of modulator with a more ideal signal amplitude modulation performance—still with a finite extinction ratio [14]. Here a distortion of the eye caused by SBS is more visible as can be seen comparing the 10 dBm cases with and without SBS influence. The distortion—which is caused when SBS creates a sign change in the pump wave amplitude during

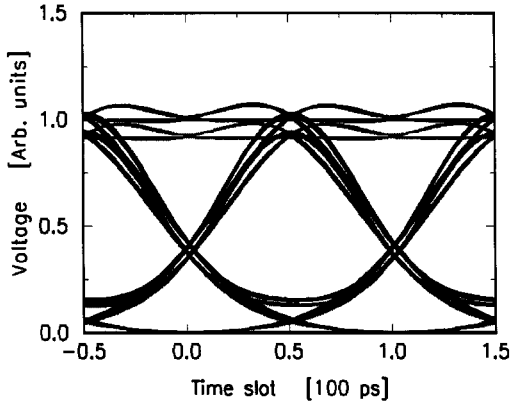

Fig. 7. Detected eye diagram after 50-km transmission using a Mach–Zehnder amplitude modulator and for an avarage input power of 2 dBm. Black (gray) curves are without (with) SBS influence.

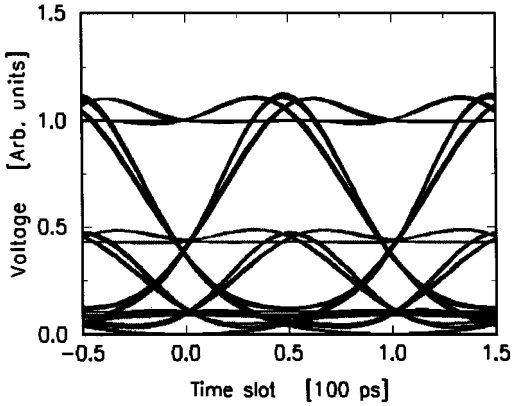

Fig. 8. Same as Fig. 7 for an average input power of 10 dBm.

OFF signal periods—is clearly identified in the bottom of the eye-diagram.

In Fig. 9, we consider for the Franz–Keldysh modulator case the influence of the detected eye under the influence of dithering of the signal with the dithering bandwidth as parameter in the situation with 10 dBm of (average) input power. It is obvious that the SBS threshold increases to above 10 dBm using a modulation bandwidth of 500 MHz (or more). Similar results are found using the Mach–Zehnder modulator.

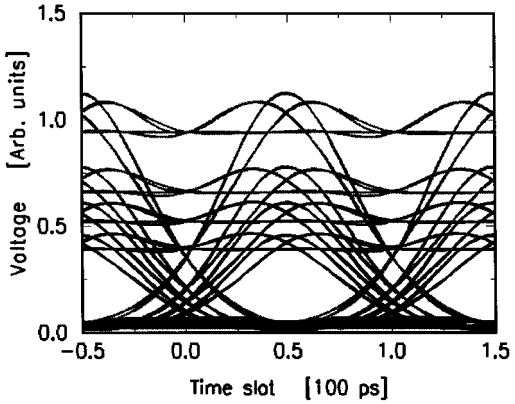

Fig. 9. Detected eye after 50-km transmission using a Franz–Keldysh absorption modulator and dithering of the signal with average signal power of 10 dBm. The dithering bandwidth is—in the order of increasing eye opening—0, 100, 200, and 500 MHz.

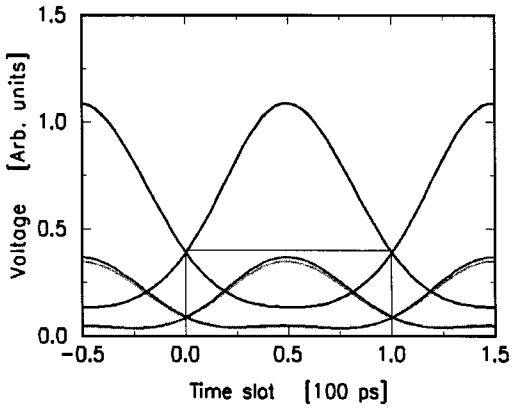

Fig. 10. Detected eye after 50 km of transmission for a sinusoidal signal modulation. Black (gray) curves are without (with) SBS influence for an average input power of 10 dBm. The frame indicates the part of the figure which is magnified in Fig. 11.

In Figs. 10 and 11, we consider as a final example a situation with sinusoidal amplitude modulation at 10 GHz, which results in an amplitude spectrum with discrete signal components separated by multiples of 10 GHz. We compare the detected eye accounting for the SBS influence on the carrier alone as well as accounting for the influence also on the four sidebands closest to the carrier on the low as well as on the high frequency side. It appears that the influence of SBS on the sidebands (that are at least 9.5 dB below the carrier at the fiber input) only causes minor changes to the detected eye.

VII. Conclusion

We present a new simplified analysis—that includes in a straightforward way the effect of spontaneous emission—of the (dynamic) influence of stimulated Brillouin scattering (SBS) on the detected receiver eye diagram. The analysis describes the main influence of SBS on the transmitted signal as that of depleting the signal carrier wave and it applies in principle for general types of modulation formats such as the digital formats of ASK, FSK, and PSK. The dynamic formulation allows in a split step numerical evaluation a determination of the signal power depletion and intersymbol-interference (ISI) caused by

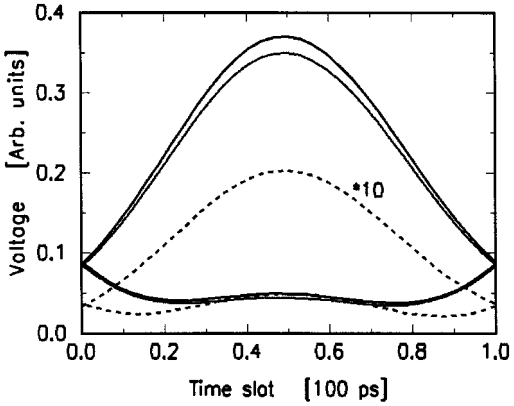

Fig. 11. The influence of considering only carrier depletion (black full curves) and to consider in addition depletion of the four nearest descrete sidebands (gray full curves) for sinusoidal modulation and an input power of 10 dBm. The dashed curves (magnified by a factor of 10) show the difference between full black and gray curves.

the combined effect of fiber dispersion, fiber attenuation and nonlinear fiber effects such as the effect of SPM and SBS.

The carrier depletion of a CW signal is in our numerical examples used to calibrate the dynamic time dependent Schrödinger equation. This is done by adjusting the spontaneous emission parameter in order to obtain a specified value for the SBS threshold. Using this value for the spontaneous emission parameter the SBS influence is uniquely given for input pump powers below, around as well as above the threshold. The analysis allows a quantification of the dithering influence on the SBS threshold.

Representative numerical examples are presented for two single-channel ON–OFF modulated 10-Gb/s systems utilizing typical Franz–Keldysh and Mach–Zehnder-type modulators. It is obvious that in the Franz–Keldysh case—where the signal modulation is imposed upon the optical signal intensity—the main effect of SBS on the detected eye is a reduction in the eye opening. In the Mach–Zehnder case—where the modulation is an ideal modulation of the optical signal amplitude—SBS may in addition to the reduction of the eye opening cause distortion of the eye shape due to SBS induced sign changes in the optical signal amplitude during the OFF signal periods.

References

[1] S. Kawanishi, H. Takara, K. Uchiyama, I. Shake, and K. Mori, "3 Tbit/s (160 Gbit/s × 16 ch) OTDM-WDM transmission experiment," in *Proc. OFC'99*, Postdeadline paper PD1.

[2] N. S. Bergano, C. R. Davidson, C. J. Chen, B. Pedersen, M. A. Mills, N. Ramanujam, H. D. Kidorf, A. B. Puc, and M. D. Levonas, "640 Gb/s transmission of sixty-four 10 Gb/s WDM channels over 7200 km with 0.33 (bits/s/)/Hz spectral efficiency," in *Proc. OFC'99*, Postdeadline paper PD2.

[3] G. P. Agrawal, *Nonlinear Fiber Optics*, 2nd ed. New York: Academic, 1995.

[4] R. W. Boyd, *Nonlinear Optics*. New York: Academic, 1992.

[5] S. Rae, I. Bennion, and M. J. Carswell, "New numerical model of stimulated Brillouin scattering in optical fibers with nonuniformity," *Opt. Commun.*, vol. 123, pp. 611–616, 1996.

[6] R. W. Boyd, K. Rzazewski, and P. Narum, "Noise initiation of stimulated Brillouin scattering," *Phys. Rev. A*, vol. 42, pp. 5514–5521, 1990.

[7] L. Chen and X. Bao, "Analytical and numerical solutions for steady state stimulated Brillouin scattering in a single-mode fiber," *Opt. Commun.*, vol. 152, pp. 65–70, 1998.

[8] R. W. Tkack, A. R. Craplyvy, F. Forghieri, A. H. Gnauck, and R. M. Drosier, "Four-photon mixing and high speed WDM systems," *J. Lightwave Technol.*, vol. 13, pp. 841–849, 1995.
[9] ITU Recommendations G.957, G.692.
[10] R. H. Inns and I. P. Batra, "Saturation and depletion in stimulated light scattering," *Phys. Lett.*, vol. 28A, pp. 591–592, 1969.
[11] R. W. Lucky, J. Salz, and E. J. Weldon Jr., *Principles of Data Communication*. New York: McGraw-Hill, 1968, ch. 8.
[12] K. Yonenaga and S. Kuwano, "Dispersion-tolerant optical transmission system using duobinary transmitter and binary receiver," *J. Lightwave Technol.*, vol. 15, pp. 1530–1537, 1997.
[13] O. Sahlén, "Optimization of DFB lasers integrated with Franz–Keldysh absorption modulators," *J. Lightwave Technol.*, vol. 12, pp. 969–976, 1994.
[14] A. Djupsjöbacka, "Residual chirp in integrated-optic modulators," *IEEE Photon.s Technol. Lett.*, vol. 4, pp. 41–43, 1992.
[15] E. M. Dianov, B. Ya. Zel'dovich, A. Ya. Karasik, and A. N. Pilipetskii, "Feasibility of suppression of steady-state and transient stimulated Brillouin scattering," *Sov. J. Quantum Electron.*, vol. 19, pp. 1051–1053, 1989.
[16] G. Grosso and A. Höök, "Generation of short pulses by stimulated Brillouin scattering in optical fibers," *J. Opt. Soc. Amer. B*, vol. 10, pp. 946–951, 1993.

A. Djupsjöbacka, photograph and biography not available at the time of publication.

G. Jacobsen, photograph and biography not available at the time of publication.

B. Tromborg, photograph and biography not available at the time of publication.